


A comprehensive investigation of histotype-specific microRNA and their variants in Stage I epithelial ovarian cancers

Angelo Velle¹  | Chiara Pesenti^{2,3} | Tommaso Grassi⁴ | Luca Beltrame⁵ | Paolo Martini⁶ | Marta Jaconi⁷ | Federico Agostinis¹ | Enrica Calura¹ | Dionyssios Katsaros⁸ | Fulvio Borella⁹ | Robert Fruscio⁴ | Maurizio D'Incalci^{10,11} | Sergio Marchini⁵ | Chiara Romualdi¹

¹Department of Biology, University of Padova, Padova, Italy

²Department of Oncology, Mario Negri Institute for Pharmacological Research, Milan, Italy

³Medical Genetics Unit, ASST Santi Paolo e Carlo, Milan, Italy

⁴Department of Obstetrics and Gynaecology, San Gerardo Hospital, University of Milano-Bicocca, Monza, Italy

⁵IRCCS Humanitas Research Hospital, Molecular Pharmacology Lab, Rozzano, Italy

⁶Department of Molecular and Translational Medicine, University of Brescia, Brescia, Italy

⁷Department of Pathology, San Gerardo Hospital, University of Milano-Bicocca, Monza, Italy

⁸Azienda Ospedaliero-Universitaria Città della Salute, Presidio S Anna and Department of Surgical Science, Gynecology, University of Torino, Torino, Italy

⁹Gynaecology and Obstetrics 1, Department of Surgical Sciences, St Anna Hospital and University of Torino, Turin, Italy

¹⁰Cancer Pharmacology, IRCCS Humanitas Research Hospital, Italy

¹¹Department of Biomedical Sciences, Humanitas University, Italy

Correspondence

Maurizio D'Incalci, Department of Biomedical Sciences, Humanitas University, Via Rita Levi Montalcini 4, 20072 Pieve Emanuele (MI), Italy.

Email: maurizio.dincalci@hunimed.eu

Funding information

Associazione Italiana per la Ricerca sul Cancro, Grant/Award Numbers: MFAG23522, IG 19997, IG 21837

Abstract

isomiRs, the sequence-variants of microRNA, are known to be tissue and cell type specific but their physiological role is largely unknown. In our study, we explored for the first time the expression of isomiRs across different Stage I epithelial ovarian cancer (EOC) histological subtypes, in order to shed new light on their biological role in tumor growth and progression. In a multicentric retrospective cohort of tumor biopsies (n = 215) we sequenced small RNAs finding 971 expressed miRNAs, 64% of which are isomiRs. Among them, 42 isomiRs showed a clear histotype specific pattern, confirming our previously identified miRNA markers (miR192/194 and miR30a-3p/5p for mucinous and clear cell subtypes, respectively) and uncovering new biomarkers for all the five subtypes. Using integrative models, we found that the 38% of these miRNA expression alterations is the result of copy number variations

Abbreviations: ACE, Absolute Copy Estimator; AIC, Akaike Information Criterion; CNV, copy number variations; COAD, colon adenocarcinoma; DEM, differentially expressed miRNA; EC, endometrioid; EOC, epithelial ovarian cancer; FDR, false discovery rate; HGSOE, high grade serous; HU, highly unstable; KIRC, kidney renal clear cell carcinoma; LGSOC, low grade serous; MOC, mucinous; OCC, clear cells; OV, ovarian serous cystadenocarcinoma; S, stable; SCNA, somatic copy number alteration; SNP, single nucleotide polymorphism; SNV, Single Nucleotide Variant; SWGS, Shallow Whole Genome Sequencing; TF, transcription factors; U, unstable; UCEC, uterine corpus endometrial carcinoma.

Angelo Velle and Chiara Pesenti contributed equally as cofirst authors.

Sergio Marchini and Chiara Romualdi contributed equally as colast authors.

This is an open access article under the terms of the [Creative Commons Attribution](https://creativecommons.org/licenses/by/4.0/) License, which permits use, distribution and reproduction in any medium, provided the original work is properly cited.

© 2022 The Authors. *International Journal of Cancer* published by John Wiley & Sons Ltd on behalf of UICC.

while the 17% of differential transcriptional activities. Our work represents the first attempt to characterize isomiRs expression in Stage I EOC within and across subtypes and to contextualize their alterations in the framework of the large genomic heterogeneity of this tumor.

KEYWORDS

biomarker, histotype, miRNA, ovarian cancer, sequencing

Whats' new?

Little is known about the molecular characteristics that distinguish the subtypes of Stage I ovarian cancer. The expression profile of microRNA (miRNA) can be used to distinguish certain subtypes and also help predict survival. Here, the authors cataloged the array of miRNA variants, called isomiRs, expressed in a cohort of Stage I epithelial ovarian cancers and investigated their biological role in tumor growth and progression. Different tumor subtypes could be distinguished by the collection of isomiRs they expressed, and many of these isomiRs result from copy number variations and changes in transcription factor activity, suggesting a role in tumor evolution.

1 | INTRODUCTION

Epithelial ovarian cancer (EOC) is one of the most lethal gynecologic diseases, with survival rate virtually unchanged over the last 30 years. Patients with disease limited to the ovary (FIGO, Stage I) represent 10% to 20% of all EOC and have a 5-years survival rate close to 80%. In contrast, when the disease is diagnosed in the upper abdomen or beyond (FIGO stages III and IV), that is the majority of cases, the survival rate is lower than 20%.¹

Although large efforts have been made to study the molecular heterogeneity of Stage III/IV, Stage I tumors have been largely overlooked, mainly because of their infrequent nature—which limits recruitment of sizable cohorts of cases—and their histological heterogeneity. Stage I encompasses five distinct histological subtypes (high grade serous, HGSOC; low grade serous, LGSOC; clear cells, OCCC; mucinous, MOC; endometrioid, EC), with different tissue of origin, peculiar genetic lesions, response and outcomes to standard treatments.² On a sizable and unique cohort of Stage I EOC our group has investigated the molecular differences that characterize each subtype and its prognosis. We demonstrated that: (i) the expression profile of a subset of miRNA acts as histotype specific biomarker for clear cell and mucinous subtypes (miR-30a-5p/3p and miR-192/194, respectively)³; (ii) miR-200c is an independent prognostic biomarker of survival⁴ and it is part of a more complex network composed of miRNAs, coding genes and lncRNAs which together predict patients relapse better than conventional classifiers based on anatomic-pathology⁵⁻⁷; (iii) each subtype can be further subclassified into three genomic profiles based on the length and the extent of somatic copy number alteration.⁸ Overall, these findings suggest that the biology of Stage I EOC is more complex than depicted by histopathological data, and that a more detailed knowledge of its molecular events is mandatory to improve patients' clinical outcome.

Several novel miRNA sequence variants (isomiRs) have been recently detected alongside their canonical counterparts with the

massive use of next generation sequencing technology. Many studies demonstrated that isomiRs are physiological events occurring in both normal and pathological tissues. IsomiRs results from enzyme mediated RNA sequence modifications and differs from the canonical sequence in length, sequence or both.⁹

A recent classification categorizes isomiRs into at least two classes. The first is characterized by the presence of single nucleotide polymorphisms (SNPs) in the canonical miRNA sequences. This modification can cause changes in miRNAs expression, processing, and functions.¹⁰⁻¹³ The second is characterized by alterations at the 5' and 3' ends generated during the miRNA maturation process.^{9,14-19} These small molecular changes in length and sequence could be responsible for seed modification, which ultimately results in a possible “targetome shifting.”²⁰⁻²² Although functional data are largely incomplete, isomiRs are expected to influence miRNAs stability^{23,24} and their subcellular localization,^{25,26} with their function not completely overlapping with that of their canonical counterparts.

Given their regulatory functions in key cellular processes and their tissue-specificity, a more comprehensive knowledge of isomiR expression in tumor seems desirable.

In our study, we profiled the entire repertoire of miRNAs and isomiRs expressed on a unique cohort of 215 Stage I EOC samples with the aim to: (i) provide the first catalog of isomiRNAs in Stage I EOC different histological subtypes; (ii) infer the molecular mechanisms, transcription factor (TF) activity and copy number variation (CNV), driving and sustaining isomiR alterations.

2 | MATERIALS AND METHODS

2.1 | Study cohort

A unique retrospective cohort of 215 snap-frozen tumor biopsies was selected from a tumor tissue collection of 225 Stage I EOC stored in

TABLE 1 Summary of the patients' clinicopathological features

Clinical annotations	Number of patients	% of patients	Number of patients with FU	Median FU [IQR 1-3]
Histology and grade				
Mucinous			38	11.2 y [7.2 y-14.3 y]
G1	26	13		
G2	10	5		
G3	1	0.5		
n.d	1	0.5		
Clear cells	28	14	26	6 y [2.8 y-14.5 y]
Endometrioid				
G1	14	7		
G2	38	19		
G3	29	14		
Low grade serous	19	9	19	14.2 y [10.4 y-17.1 y]
High grade serous	37	18	35	7.3 y [5.3 y-16.3 y]
FIGO substages				
A	68	33		
B	14	7		
C	117	58		
n.d	4	2		
Median age at diagnosis [min-max];	54.9 y [16.5 y-89.3 y]			
Chemotherapy				
Yes	146	72		
No	51	25		
n.d	6	3		
Relapse				
Yes	43	21		
No	147	72		
n.d	13	7		
OS [IQR 1-3]	10.1 y [6.2 y-15.5 y]			
PFS [IQR 1-3]	8.7 y [4.9 y-14.5 y]			
Total number of patients	203			

Abbreviations: FU, follow-up; G, grade; OS, overall survival; PFS, progression free survival.

Pandora biobank at IRCCS Istituto di Ricerche Farmacologiche Mario Negri (Milano, Italy) (Table 1) as previously published.^{3-7,27} Patients were enrolled from two independent Italian clinical centers: 172 from San Gerardo Hospital (Monza, Italy), and 53 from Sant'Anna Hospital (Torino, Italy) from 1989 to 2018. All the samples were revised by an independent pathologist following the current guidelines of the World Health Organization for EOC.²⁸

2.2 | RNA extraction

Total RNA enriched in miRNA fraction was purified from all the snap-frozen tumor samples using the miRNeasy kit (Qiagen, Hilden, Germany), starting from about 25 mg of tissue biopsies. The procedure was carried out exploiting the automatic nucleic acid purification platform QIAcube (Qiagen, Hilden, Germany). The quantity and

the quality of the purified RNA were evaluated with Qubit RNA Broad Range High Sensitivity Assay Kit (Invitrogen, Carlsbad, CA) and 4200 TapeStation (Agilent Technologies, Santa Clara, CA), respectively.

2.3 | miRNA library preparation and sequencing

miRNA sequencing was carried out on the snap-frozen samples using the QIAseq miRNA Library kit (Qiagen, Hilden, Germany) starting from 100 ng of purified RNA.

In each sequencing experiment, 48 libraries were pooled together and sequenced on NextSeq 500 in 1 × 75 base pair (bp) mode (Illumina, San Diego, CA). The sequencing coverage and quality statistics for each sample are summarized in Supplementary Table S1.

2.4 | RNA-seq data preprocessing

Reads were trimmed using Atropos,²⁹ removing the adapters only when the overlap between the adapter and the read was at least eight bases. Only reads with at least 17 bp were used for the following analyses. Trimmed reads were aligned to hairpins with Bowtie³⁰ (v 1.2.3) using the following parameters: -k 50 -a --best --strata -e 99 999 --chunkmbs 2048 -q --seed 123 456. The Bowtie index was built starting from human hairpins fasta file available at miRBase. After the alignment, isomiRs detection and quantification was performed exploiting the mir-top³¹ pipeline using the miRBase gff3 file³² (miRBase v22).

The raw counts were annotated using isomiRs R package, assigning to each isoform a specific name following this nomenclature: “miRNA_name;isotype:nucleotide_change,”³³ lowercase nucleotides changes indicate that the base is lost in comparison to the reference sequence, otherwise the nucleotide is included. For normalization and batch correction we exploited the RUVSeq R package.³⁴ Under the assumption that the two batches (namely the two independent clinical centers) should not be different in terms of miRNA expression, we provide as negative controls the list of the top 60 differentially expressed genes between batches setting to three the number of normalization factors. Finally, miRNAs were filtered to have at least five counts in at least 10% of the samples. To compare longitudinal and bilateral samples we used the most variable genes defined as the top 100 genes ordered by SD.

2.5 | Differential analysis and biomarker detection among the five Stage I EOC histotypes

To identify the differentially expressed miRNA (hereafter called DEM) we used the edgeR R package.³⁵ We provided as input the filtered raw counts with the design matrix defined by the dicotomous variables for the histotypes and the three estimated RUV factors for data normalization and batch correction (see Section 2.4). False discovery rate (FDR) less than 0.05 was used to select significant miRNA.

To identify among the list of DEM the biomarker miRNA (defined as those miRNA with a high predictive role) for each histotype, we implemented a resampling-based inferential algorithm in three steps: (1) random selection of 70% of the samples (keeping the proportions among histotypes); (2) identification of differentially expressed miRNA among the five histotypes (FDR < 0.1); (3) Selection of isomiRs which are significantly overexpressed in one histotype in respect to each of the others. These steps have been repeated 1000 times and only isomiRs selected in at least 800 resampling have been selected as histotype markers.

2.6 | miRNA and isomiRNA target prediction

PITA miRNA target prediction tool³⁶ was used to study target variations among different miRNA isoforms. We provided the list of 3' UTR sequences of all known genes as potential targets and the sequences of histotype markers and differentially expressed isomiRs

as potential regulators. Default options were used. Finally, the candidate targets (with a cutoff of -9 for PITA) of a given isomiR were compared to the targets of the corresponding reference miRNA. ClusterProfiler Bioconductor package³⁷ has been used to identify significantly enriched pathways within each list of targets.

2.7 | Shallow Whole Genome Sequencing (sWGS) data analysis and integration

KAPA HyperPrep kit was exploited to perform low coverage whole genome sequencing (sWGS) and experiments were run according to the manufacturer's instructions (Roche, Basel, Switzerland). In those cases where tumor content cannot be evaluated by the pathologist, the Absolute Copy Estimator (ACE) tool was used to infer the tumor purity and ploidy of each sample based on the results of Single Nucleotide Variants (SNVs) calls obtained from an in house designed panel of 139 coding genes. Absolute SCNAs profiles within each histotype were analyzed by Genomic Identification of Significant Targets in Cancer algorithm (GISTIC). The sequencing quality statistics for each sample are summarized in Supplementary Table S2.

2.8 | Copy number variation and expression integration

The copy number status was quantified using the segment mean value returned by the Absolute Copy number Estimator (ACE) software.³⁸ This value represents the expected number of copies for a given genome segment, and this value is assigned to all genes contained in the segment. For all miRNAs found at different loci, the final copy number status is obtained by calculating the sum of the copy number status of the loci.

To study the association between isomiR expression and their copy number status, we used a generalized linear model as implemented in the edgeR R package. We estimated a model for each miRNA where the raw miRNA counts were the independent variable and the copy number values across samples and the RUV factors for the normalizations were used as covariates. Likelihood ratio test was used to test the significance of the parameter associated with the SCNA variable, a significant estimate means a significant association between isomiR expression and its CNV. For this analysis the miRNA expression has been considered the ensemble of its isotypes.

IsomiRs with pvalue < 0.1 and with a positive coefficient were defined as significant and concordant: the higher the CNV the higher the expression.

2.9 | Transcription-target (TF)-miRNA interactions

To study the relationship between the expression of TFs and their target miRNAs, we used microarray expression data for a subset of 65 samples of our cohort⁷ (E-MTAB-1814). The literature-curated relationships

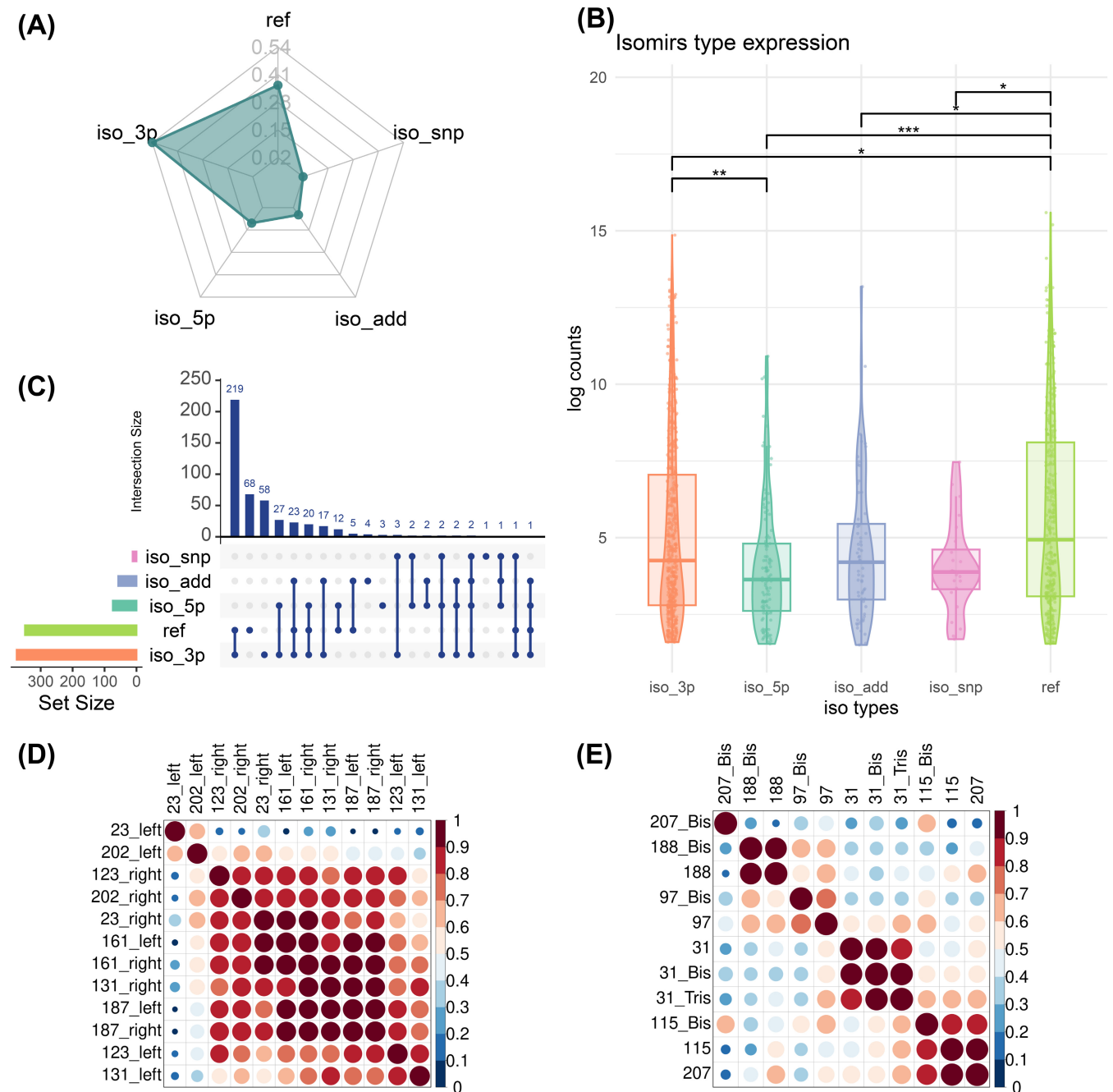


FIGURE 1 (A) Radar plot representing the distribution of expressed isomiRs among isotypes. The axis shows the fraction of expressed isomiRs belonging to a given isotype. (B) Distribution (in terms of boxplots and violin plots) of the log₂ average expression of isomiRs for the five isotypes. For each isomiR the average of the normalized expression has been calculated across all samples. (C) The UpSet plot represents the intersection between the sets of miRNA expressing a given isotype. The vertical bar plot reports the intersection size, the dot plot reports the set participation in the intersection, and the horizontal bar plot reports the set sizes. Correlation plot for bilateral cases (D) and relapses (E). The correlation between two samples is computed on the 100 most variable isomiRs. The circle dimension and color represent the values of correlation

TF-miRNA were downloaded from the TransmiR database³⁹ (v2.0). And, to infer the impact of TF on miRNA expression we used a linear regression model for each miRNA. The model included the miRNA expression profile as the dependent variable, and the TFs as the independent covariates. To remove the effect of CNVs on miRNA expression we take the standardized residual inferred from CNV-expression models as described in the previous paragraph. miRNAs

can be regulated by many TFs so, for each miRNA, we removed from the model the TFs with the weakest association using an automatic stepwise regression strategy as implemented in the stepA function. Stepwise regression selects the best predicting variables starting from the full model (including all the TFs) and removing backward one variable at a time comparing the AIC (Akaike Information Criterion) values. For each model we selected the TFs with pvalue < 0.05.

3 | RESULTS

3.1 | Cohort description

To achieve the aims of the study, a retrospective cohort of 215 snap-frozen tumor biopsies was obtained from 203 patients with diagnosis of Stage I EOC. The cohort was composed of 209 samples obtained at primary surgery, from patients who had not received chemotherapy (43 HGSOC, 21 LGSOC, 83 EC, 30 OCCC and 38 MOC). Six samples were from matched bilateral tumors. Additional cases were from matched biopsies withdrawn at relapse. The demographic and clinical features (Table 1) show that the study cohort is histologically distributed and, representative of the clinical situation.^{5,8,27}

3.2 | miRNA landscape profiling by NGS

To profile the entire repertoire of expressed miRNAs in our cohort (Table 1), including reference miRNAs and isomiRs (with sequence variations), short mRNA libraries of tumor biopsies were sequenced and analyzed (see Section 2).

After data preprocessing and filtering, we detected 971 miRNAs, 349 (36%) of which were classified as reference miRNA (defined as ref) and 622 (64%) as miRNA variants. The radar plot reported in Figure 1A shows that the majority of miRNA modifications (54%) accounted for the addition or deletion of nucleotides at the 3'-end (iso_3p) while 12% for the addition or deletion of nucleotides at the 5'-end (iso_5p). The presence of mismatch (iso_snp) as well as the addition of one or more nucleotides not present in the precursor sequence (iso_add) accounted for a small part of isomiRs (2% and 6%, respectively). This distribution and the type of modification were maintained across the different histological subtypes as detailed in Supplementary Results section 1 and in Supplementary Figures S1-S3.

Considering the total amount of miRNAs expressed, we counted 208 miRNAs as expressed in all the samples (of these 95 are reference, 103 are iso_3p, four are iso_5p, eight are iso_snp), while 444 miRNAs are expressed in at least 80% of the samples. The reference, the iso_3p and the iso_add miRNAs are characterized by a significantly higher average expression with respect to iso_snp and iso_5p (Figure 1B), demonstrating that these miRNA types are abundant and potentially functional in our samples. Finally, we observed that the majority of miRNAs ($n = 236$) expresses the reference and one type of isomiR (Figure 1C).

3.3 | Bilateral and longitudinal samples are characterized by the same repertoire of miRNA variants

Taking advantage of the presence in our cohort of matched bilateral biopsies (for two LGSOC, three HGSOC and one OCCC patients) and longitudinal matched biopsies (for two EC, three HGSOC and one OCCC patients), we explored whether isomiRs expression exhibited

spatial and temporal correlation. Using the selection of the most variable and highly expressed isomiRs we performed a pair-wise correlation analysis (Figure 1D,E) separately for bilateral (Figure 1D) and longitudinal samples (Figure 1E). While bilateral samples, except for sample 23, show a high degree of correlation within ($r = 0.85$) and among patients ($r = 0.76$), longitudinal samples, apart from sample 207, show a strong within-patient ($r = 0.84$) but a low interpatient similarity ($r = 0.49$). These observations suggest that the global expression profile of reference miRNAs and of their isomiRs is a molecular fingerprint for each Stage I EOC tumor biopsy.

3.4 | isomiRs as histotype specific biomarkers

We next questioned whether the different histological subtypes are characterized by a different expression of miRNAs. We initially aimed at identifying those miRNAs that resulted as differentially expressed (DEM) among the five main histological subtypes.

Globally, we identified 686 DEM derived from 367 different miRNAs loci. Among them, 37% are reference and 63% are isomiRs (iso_3p = 53.3%, iso_5p = 10.5%, iso_add = 6%, iso_snp = 1.6%) (Supplementary Results section 2, Supplementary Figures S4 and S5).

Although DEMs have significant adjusted *P*-value, due to sample variability, only few of them can be exploited as subtype specific biomarkers, that is, miRNAs with high predictive potential.

Using a resampling-based strategy (see Section 2) we found 42 histotype-specific miRNAs, nine of which were specific to HGSOC, three to LGSOC, seven to EC and OCCC, and 16 to MOC subtypes (Figure 2A and Supplementary Table S3).

Reference miR192/194 and miR30a-3p/5p were previously identified as specific biomarkers of MOC and OCCC subtypes in a largely overlapping cohort exploiting microarray data for expression profiling. It is noteworthy that these miRNAs were confirmed as tissue specific biomarkers in our sequencing-based study, supporting confidence in the robustness of our analysis. However, NGS data analysis revealed that these four reference miRNAs are coexpressed with at least one additional variant. In particular, miR-30a-3p expressed an histotype specific iso_add (hsa-miR-30a-3p;iso_add:T) while the other miRNAs were characterized by histotype specific iso_3p modifications. The complete list of biomarkers with their different histological subtype is reported in Supplementary Table S4.

The high predictive potential of the 42 biomarkers is reflected by the clustering shown in Figure 2B. Except for EC samples that still show a high degree of variability, MOC, LGSOC and OCCC are almost perfectly classified using the 42 biomarker profiles, such classification is clearly superior to that based on the list of DEM (Supplementary Figure S4D).

3.5 | isomiRs' tumor and tissue specificity

miRNA expression profiles are known to be tightly regulated in a tissue specific manner both in physiological and pathological conditions.

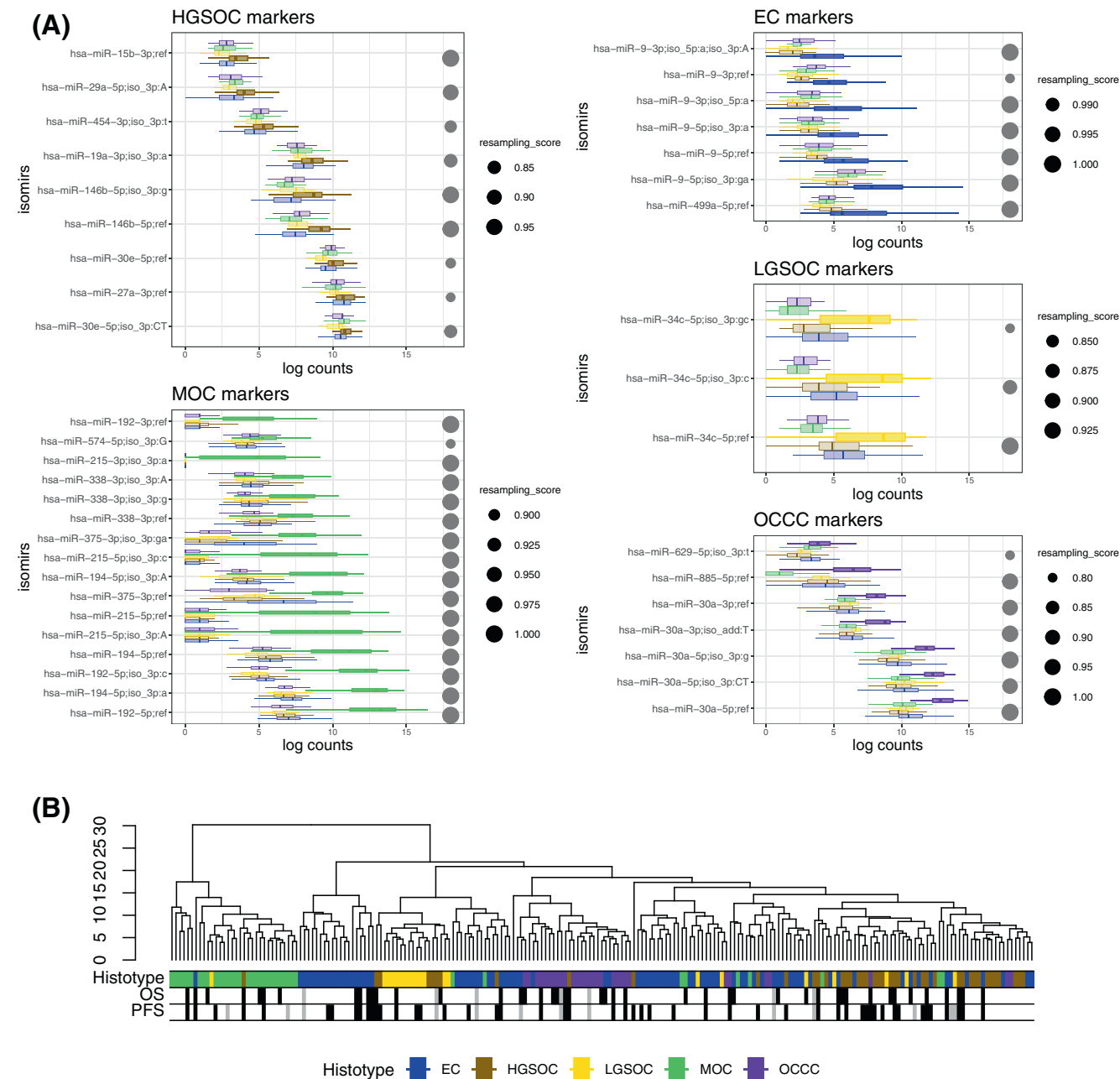


FIGURE 2 (A) Expression distribution (boxplots) of histotypes' markers. The X axis represents the expression level of the isomiRs, while the Y axis represents the different iso-markers. For each marker a boxplot of each histotype is shown. The dimension of the dots on the right of each plot represents the resampling score detection algorithm, greater the dots, higher the score. (B) Dendrogram showing the hierarchical clustering of markers' expression. The clustering has been computed on the Euclidean distances using the complete linkage. The annotation bars represent histotypes, OS and PFS, respectively. For OS and PFS annotation bars, black and white represent the presence and absence of an event, respectively, while gray represents unknown status

With the aim of exploring isomiR tissue specificity in Stage I EOC we performed two different analyses. In the first we investigate the expression levels of our biomarkers in other solid tumors. In the second, we compare the expression of LGSOC and HGSOC isomiR biomarkers with their expression in normal fallopian tubes. While the first analysis explores tissue specificity, the second tries to shed new light on the possible tissue of origin for the serous histotype, both at low and high grade.

From the Tumor IsomiR Encyclopedia (TIE) we selected Ovarian serous cystadenocarcinoma (OV), Uterine Corpus Endometrial Carcinoma (UCEC), Kidney Renal Clear Cell Carcinoma (KIRC) and Colon Adenocarcinoma (COAD) samples as they affect the tissue types that correspond to our histotypes. Data reported in Figure 3A show the average expression (color of the dots) and the frequency of detected expression (dimension of the dots) in the TCGA cohorts. Our results indicate that almost all histotype-specific biomarkers are expressed in

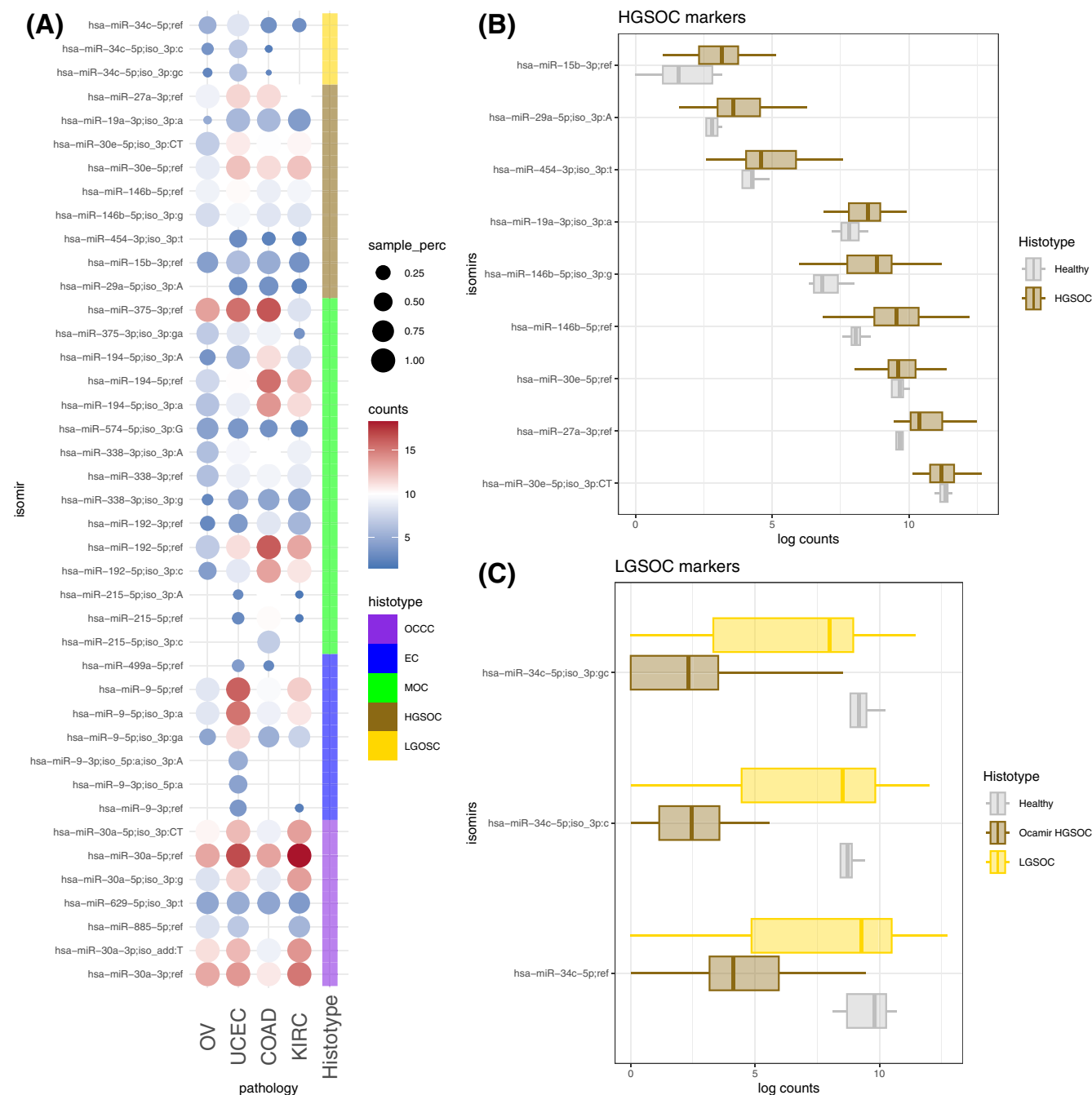


FIGURE 3 (A) Expression of histotype markers in selected advanced stage tumors taken from the TCGA. IsomiRs are represented on the Y axis and tumors on the X axis. The color of the dots represents the log₂ of isomiRs' mean expression in a given tumor. The dimension of the dots represents the fraction of samples that expresses the isomiR. The annotation bar on the right shows the histotype-specificity of each isomiR. (B) Comparison between the expression of HGSOC markers in tumors and healthy fallopian tubes. IsomiRs are shown along the Y axis, while the X axis represents the log expression. (C) Comparison between the expression of LGSOC markers in LGSOC samples, OCAMIR's HGSOC samples and healthy fallopian tubes. IsomiRs are shown along the Y axis, while the X axis represents the log expression

other solid tumors with a clear tumor specificity (Figure 3A). Specifically, isomiRs of miR-9, reported as EC markers, are found expressed only in UCEC samples, while isomiRs of miR192/194, miR-215 and miR-375 family, known to be MOC markers, are found expressed prevalently in COAD samples. isomiRs of miR-30a family are widely expressed but with a preferential expression in KIRC samples.

These results highlight the high degree of tissue specificity of our biomarkers, a characteristic that is widely accepted for most miRNAs, and provide interesting hints as to how tumors with the same histotype from different sites may evolve.

While for HGSOC the tubal paradigm is the most plausible, the origin of LGSOC remains under debate, they are thought to arise from

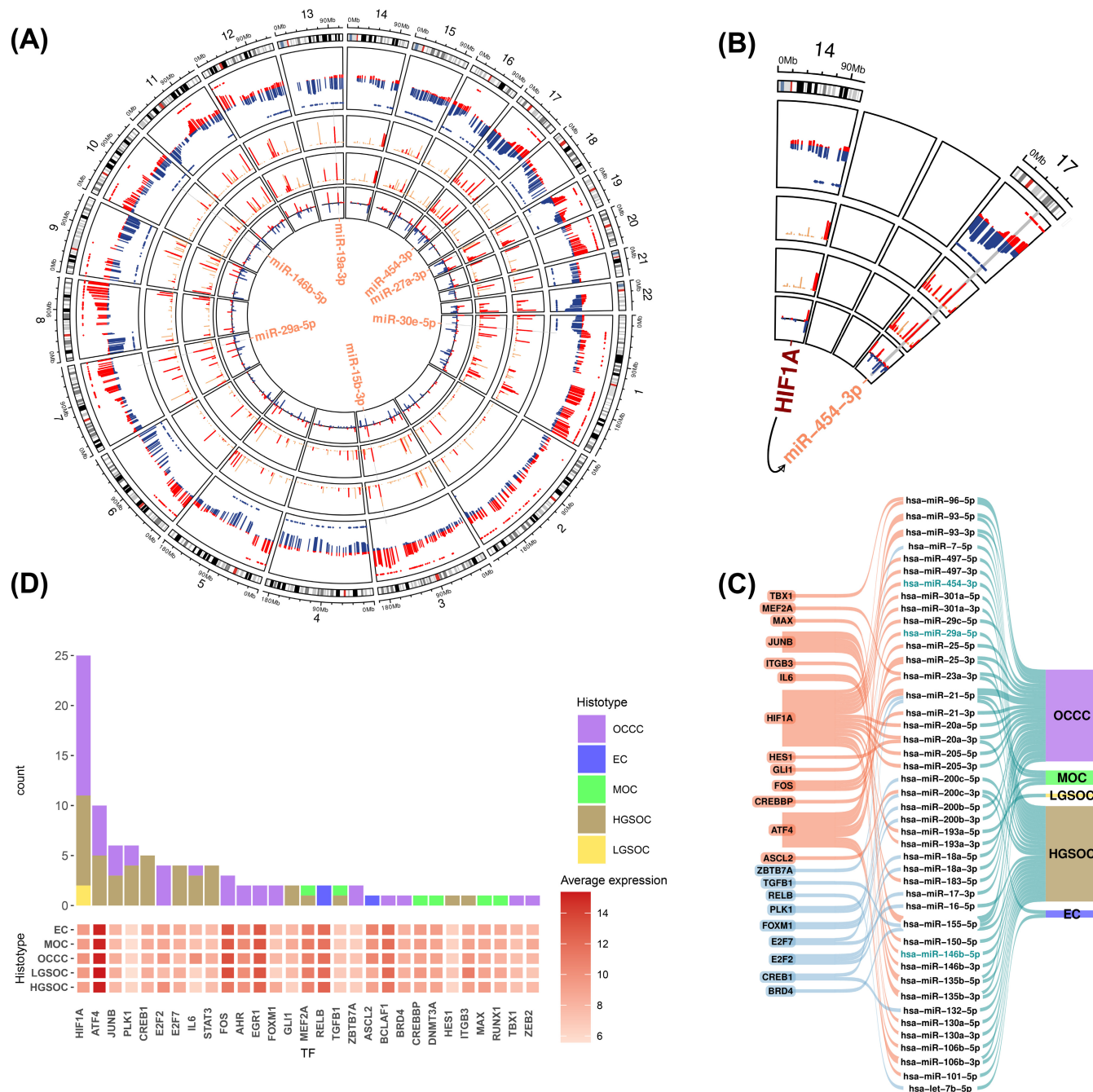


FIGURE 4 Circos plots summarizing multiomics data on a genomic scale for HGSOc samples (A) and the zoomed version for chromosome 14 and 17 (B). (A and B) In the first (external) layer the fraction of samples with amplification (red) or deletion (blue) for each miRNA is shown. Dots at the extremities of the layer highlight miRNA whose fraction of amplified/deleted samples is above the average value. The second and third layer represent the expression levels of the reference and of the iso_3p isoforms, respectively. Isoforms whose expression is significantly and concordantly associated to CNV status are highlighted with a brighter red color. In the fourth layer the ratio between reference and iso_3p expression is represented. The black baseline correspond to 0, positive values are displayed in red while negative in blue. At the center of the plot the position of markers is highlighted. (C) Alluvial plot showing the multi-to-multi relationships between TF and DEM along with their histotype specificity. TF are represented in the first column, significantly targeted DEM in the second column, histotypes in which the relationship is highly correlated in the third column. Red lines represent positive regulation for the TF-miRNA couple while blue represent negative regulation. (D) Barplots (upper part) showing the number of different miRNAs that a TFs transcriptionally regulate (with their contribution within each histotype) and heatmap (lower part) showing their average expression in the five histotypes

fallopian tubes or from the ovarian surface epithelium.⁴⁰⁻⁴³ To explore the similarity of the expression of HGSOc and LGSOC biomarkers with that in their putative tissue of origin, we exploited the data

available from the OCaMIR signature⁴⁴ (GSE127873) where miRNA-seq data have been generated for both healthy fallopian tubes and early stage ovarian tumor samples. Data reported in Figure 3B,C,

shows that (i) our biomarkers are found expressed in healthy fallopian tubes, that (ii) seven out of nine HGSOC markers (miR-15b-3p;ref, miR-29b-5p;iso_3':A, miR-454-5p;iso_3':t, miR-19a-3p;iso_3':a, miR-146b-5p;ref, miR-146b-5p;iso_3':g, miR-27a-5p;ref) have a significant higher expression in tumor samples with respect to healthy tissue, confirming their diagnostic and predictive potential and that (iii) all the three biomarkers of LGSOC (miR-34c-5p;ref and its variants) are expressed at comparable levels between tumor and normal epithelial fallopian tube, but with a significantly higher expression with respect to their HGSOC counterpart.

In conclusion, our data indicate that biomarkers of low- and high-grade serous tumors are found expressed in healthy fallopian tubes suggesting that, although characterized by different evolutionary paths, as highlighted by the heterogeneous isomiR distribution between low and high grade, the tubal paradigm can explain the common origin of serous subtypes.

3.6 | Integration of miRNA expression and copy number alterations

We have recently demonstrated that Stage I EOC is molecularly characterized by three different genome instability patterns (namely stable, S, unstable, U and highly unstable, HU) lagging each histological subtype.⁸ As genome structural rearrangements can be, at least in part, a plausible mechanism for miRNA expression alterations, we integrated miRNA and SCNA profiles to question whether the increased expression of previously identified miRNAs could be the result of structural changes in their genomic loci. To this aim, we implemented a regression-based model to estimate the association between the CNV profiles⁸ and the miRNA expression profiles. Briefly, we considered that if the over/underexpression of a miRNA is the result of a genomic event (ie, amplification/deletion) a significant and concordant association would be expected.

Circos plots reported in Figure 4A summarize the results of the integrative analysis obtained on the entire list of expressed miRNAs in HGSOC samples. Figure 4A and its zoom in Figure 4B show, for each genomic loci in which we identified an expressed miRNA, the proportion of patients with an event of amplification/deletion (first layer, respectively red and blue bars), the average expression of the reference miRNA and of its iso_3p variant (second and third layers, in bright red those miRNAs with expression significantly associated with their CNV levels), and of their expression ratio in log scale (the most inner layer). At the center of the circos we highlighted the genomic position of the HGSOC biomarkers. The same plots for all the other histotypes are available in Supplementary Figure S6, while the complete list of miRNAs whose expressions have a significant and concordant association with CNVs are available in Supplementary Table S5.

We found 209 miRNAs whose expression level is significant and concordant with their CNV. Of these, 141 are DEM. This means that 38% (141 over 367) of miRNA transcriptional deregulations are the result of genomic instability. Among these 141 we found 11 biomarkers: two are biomarkers of EC (miR-9-3p/5p), one of MOC (miR-

574-5p), six of HGSOC (miR-19a-3p, miR-27a-3p, miR-15b-3p, miR-29a-5p, miR-454-3p and miR-30 e-5p) (Figure 4A), two of OCCC (miR-30a-3p/5p). Since our markers derive from 23 canonical miRNAs, our results suggest that 48% (11 over 23) of the markers are highly expressed because of genomic instability.

Taken together our results suggest that more than a third of the differential expression observed (and half of the biomarkers), is due to heterogeneity in terms of genome instability characterizing different subtypes.

3.7 | Transcriptional regulation of isomiRs

Differential TF activity is another molecular mechanism responsible for the altered expression of miRNAs. Since miRNA alterations can be partially explained by CNVs we explored whether these differences could be also ascribed to histotype-specific transcriptional regulation activity.

To this end we exploited the expression of a list of transcription factors (TFs) known to be regulators of miRNAs (TransmiR v2.0 database) available for a subset of our cohort ($n = 65$)⁷ and used a multivariate regression model to infer TF-miRNA interactions (see Section 2 for details).

Our analysis identified 64 DEMs (17%) suggested to be transcriptionally regulated by 29 TFs. Figure 4C shows the list of the top 60% most significant TFs-miRNA relationships for each histotype (see Supplementary Table S6 for the complete list). HGSOC and OCCC are the two subtypes with the highest number of miRNAs with significant TF regulation. Interestingly, Figure 4D highlights that HIF1A, ATF4 and PLK1 are the three TFs showing the highest putative activity in both OCCC and HGSOC, in particular HIF1A and ATF4 have a high expression in our samples. While HIF1A and ATF4 act predominantly as activators, PLK1 seems to be an inhibitor of the miRNA expression. Moreover, CREB1 and IL6 have high activity (inhibitor and activator, respectively) only in HGSOC samples while JUNB, E2F2 and FOS act prevalently in OCCC samples. Among the miRNA regulated by TFs we found 4 biomarkers (1 for MOC and 3 for HGSOC). Regarding HGSOC markers, HIF1A regulates miR-454-3p (Figure 4B), IL6 regulates miR-146b-5p and GIL1 is associated with miR-29a-5p (Supplementary Figure S6E). Interestingly, miR-454-3p, CREB1, ATF4 were already identified as a biomarker of platinum resistance in HGSOC.^{45,46}

Our results show that miRNA expression is the result of a complex interplay between different forces, among which CNV and TFs play a key role.

4 | DISCUSSION

It is now widely recognized that miRNA genes express multiple isoforms (isomiR) in a tissue-specific manner in physiological or pathological conditions. Some of the isoforms of a given miRNA may differ by a single nucleotide, so their identification could occasionally be the result of both biological and technical noise. However,

the histotype-dependent expression of our DEMs suggests that at least part of the isomiRs are finely tuned in terms of expression as highlighted by our integration models. Although large efforts have been made to study canonical and noncanonical miRNA profiles in late-stage ovarian cancer^{3,4,7,47} to the best of our knowledge, the work presented here is the first attempt to profile the entire repertoire of isomiR across the different histological subtypes that characterize Stage I EOC.

Consistent with the literature, we found that the iso_3p type is the most abundant modification among the expressed isomiRs, and that many variations, along with their reference miRNAs, are characterized by histotype-dependent expression.

We confirmed our previously identified miRNA biomarkers for MOC (miR-192/194 cluster) and OCCC (miR-30a-3p/5p) and we observed that some isoforms of these miRNA markers are themselves markers as well. Moreover, we expanded the repertoire of histotype-specific markers for all the other histotypes. Specifically, miR-34c (the reference form) together with two of its iso_3p modifications are the only markers for LGSOC. An extensive body of literature shows that miR-34c is often subjected to severe alterations in various cancer models,⁴⁸⁻⁵⁰ and that its expression is fine-tuned by several tumor-suppressive pathways. miR-34c has been reported to induce cell apoptosis and to inhibit cell proliferation and invasion in a variety of tumor cells,^{51,52} consistent with the favorable prognosis of LGSOC compared to that of the other subtypes.

HGSOC is characterized by nine markers corresponding to five miRNAs (miR-146b, miR-30 e, miR-15b, miR-19a, miR-29a). Exploring the expression of these biomarkers in a collection of healthy fallopian tubes we observed that miR146b-5p and its isoforms are weakly expressed in healthy tissue, supporting their tumor-cell specificity. All these miRNAs have been found to be deregulated in many cancers. In particular, miR-146b downregulation inhibits cell migration and invasion and increased cell proliferation improving the response of EOC to chemotherapeutic agents.⁵³ In contrast, miR-19a negatively regulated the expression of PTEN and promoted the growth of ovarian cancer cells.⁵⁴

Finally, EC samples are characterized by a high expression of miR-9 and miR-499. Although its role in tumors appears to be controversial, aberrant expression of miR-9 is reported in different tumors, and it was shown to be a prometastasis onco-miR in breast cancer.⁵⁵

These isomiR markers tend to be highly tumor specific: MOC markers are highly expressed in COAD samples, OCCC markers in KIRC, EC biomarkers in UCEC. LGSOC and HGSOC biomarkers were moderately expressed in late-stage ovarian cancer samples.

Looking at the isomiR spatial and temporal expression we observed that, at the relapse, tumor samples tend to maintain a patient specific fingerprint, while, at the diagnosis, tumor samples tend to be more similar within and across patients.

A final consideration regards the mechanism of miRNA deregulation in Stage I EOC. In the present study we have investigated two possible mechanisms, such as structural alterations and TF activity. By integrating SCNA profiles, TF expression and miRNA-seq data we found that almost 38% of the expression profile

modifications are the result of SCNAs, while 17% are the result of differential TF activity. This result suggests that the differential expression among and within histotypes is mostly due to aberrant genomic copy number status. Among the miRNA markers the expression of which is modified by their SCNA we found miR-9, for EC, miR-30a for OCCC, miR-574-5p for MOC and the six HGSOC markers (miR-15b-3p, miR-454-3p, miR-29a-5p, miR-30 e-5p, miR-19a-3p and miR27a-3p).

Taken together our results indicate a heterogeneous transcriptional picture within and among histotypes. The finding that different isomiRs are generated in different histological subtypes, suggests that the production of multiple highly similar isomiRs is an inevitable consequence of the tumor evolutionary process and that isomiRs can act cooperatively with miRNAs to control functionally related genes in the establishment of different tumor cells.

AUTHOR CONTRIBUTIONS

Angelo Velle: Conceptualization, Data Curation, Formal Analysis, Methodology, Software, Visualization, Writing—original draft, Writing—review & editing. **Chiara Pesenti:** Conceptualization, Data Curation, Investigation, Methodology, Writing—review & editing. **Tommaso Grassi:** Resources and Investigation. **Luca Beltrame:** Data Curation, Investigation, Methodology, Writing—review & editing. **Paolo Martini:** Formal Analysis, Methodology, Software, Writing—review & editing. **Marta Jaconi:** Data Curation, Resources, Writing—review & editing. **Federico Agostinis:** Methodology, Software. **Enrica Calura:** Methodology, Writing—review & editing. **Dionysios Katsaros:** Data Curation, Resources, Investigation, Writing—review & editing. **Fulvio Borella:** Data Curation, Resources, Investigation, Writing—review & editing. **Robert Fruscio:** Data Curation, Investigation, Resources, Writing—review & editing. **Maurizio D'Incalci:** Conceptualization, Funding Acquisition, Project Administration, Supervision, Writing—original draft, Writing—review & editing. **Sergio Marchini:** Conceptualization, Funding Acquisition, Supervision, Project Administration, Writing—original draft, Writing—review & editing. **Chiara Romualdi:** Conceptualization, Funding Acquisition, Project Administration, Investigation, Methodology, Software, Supervision, Writing—original draft, Writing—review & editing. The work reported in the paper has been performed by the authors, unless clearly specified in the text.

ACKNOWLEDGMENT

Open access funding provided by BIBLIOSAN.

FUNDING INFORMATION

This work was supported by the IG grant to Chiara Romualdi (Grant N. IG 21837), by the IG grant to Sergio Marchini (Grant N. IG 19997) and by the “My First AIRC grant” to Enrica Calura (MFAG 2019, Grant N. 23522) all provided by Italian Association for Cancer Research (AIRC). The “Alessandra Bono Foundation” supported young investigators fellowships and the genomic infrastructure of the Cancer Pharmacology group at IRCCS Humanitas Research Hospital.

CONFLICT OF INTEREST

The authors declare that they have no known competing financial interests or personal relationships that could have appeared to influence the work reported in this paper.

DATA AVAILABILITY STATEMENT

Shallow Whole Genome Sequencing data have been submitted to European Genome-Phenome Archive (EGA; ID EGAS00001004961) and are available under controlled access. Small RNA Sequencing data are available at the European Genome-Phenome Archive (EGA; ID EGAS00001006617). Data sources and handling of publicly available data are described in Section 2. Further information is available from the corresponding author upon request.

ETHICS STATEMENT

The study was performed following the Declaration of Helsinki and written informed consent was obtained from all patients enrolled in the study. The scientific ethical committee "Brianza" approved collection and usage of tumor, blood and plasma samples (N° 1065, on November 10th, 2015, amended on February 22nd, 2018).

ORCID

Angelo Velle  <https://orcid.org/0000-0002-4010-6390>

REFERENCES

- Ferlay J, Steliarova-Foucher E, Lortet-Tieulent J, et al. Cancer incidence and mortality patterns in Europe: estimates for 40 countries in 2012. *Eur J Cancer Oxf Engl* 1990. 2013;49(6):1374-1403. doi:10.1016/j.ejca.2012.12.027
- Leskela S, Romero I, Cristobal E, et al. The frequency and prognostic significance of the histologic type in early-stage ovarian carcinoma: a reclassification study by the Spanish Group for Ovarian Cancer Research (GEICO). *Am J Surg Pathol*. 2020;44(2):149-161. doi:10.1097/PAS.0000000000001365
- Calura E, Fruscio R, Paracchini L. miRNA landscape in stage I epithelial ovarian cancer defines the histotype specificities. *Clin Cancer Res*. 2013;19(15):4114-4123. doi:10.1158/1078-0432.CCR-13-0360
- Marchini S, Cavalieri D, Fruscio R, et al. Association between miR-200c and the survival of patients with stage I epithelial ovarian cancer: a retrospective study of two independent tumour tissue collections. *Lancet Oncol*. 2011;12(3):273-285. doi:10.1016/S1470-2045(11)70012-2
- Martini P, Paracchini L, Caratti G. lncRNAs as novel indicators of patients' prognosis in stage I epithelial ovarian cancer: a retrospective and multicentric study. *Clin Cancer Res J Am Assoc Cancer Res*. 2017; 23(9):2356-2366. doi:10.1158/1078-0432.CCR-16-1402
- Calura E, Martini P, Sales G. Wiring miRNAs to pathways: a topological approach to integrate miRNA and mRNA expression profiles. *Nucleic Acids Res*. 2014;42(11):e96. doi:10.1093/nar/gku354
- Calura E, Paracchini L, Fruscio R. A prognostic regulatory pathway in stage I epithelial ovarian cancer: new hints for the poor prognosis assessment. *Ann Oncol J Eur Soc Med Oncol*. 2016;27(8):1511-1519. doi:10.1093/annonc/mdw210
- Pesenti C, Beltrame L, Velle A, et al. Copy number alterations in stage I epithelial ovarian cancer highlight three genomic patterns associated with prognosis. *Eur J Cancer Oxf Engl*. 1990;2022(171):85-95. doi:10.1016/j.ejca.2022.05.005
- Michlewski G, Cáceres JF. Post-transcriptional control of miRNA biogenesis. *RNA*. 2019;25(1):1-16. doi:10.1261/rna.068692.118
- Zhang H, Su YL, Yu H, Qian BY. Meta-analysis of the association between Mir-196a-2 polymorphism and cancer susceptibility. *Cancer Biol Med*. 2012;9(1):63-72. doi:10.3969/j.issn.2095-3941.2012.01.012
- Ghanbari M, Sedaghat S, Looper HWJ. The association of common polymorphisms in miR-196a2 with waist to hip ratio and miR-1908 with serum lipid and glucose: association of miRNA-SNPs with cardiometabolic traits. *Obesity*. 2015;23(2):495-503. doi:10.1002/oby.20975
- Carter H, Marty R, Hofree M. Interaction landscape of inherited polymorphisms with somatic events in cancer. *Cancer Discov*. 2017;7(4): 410-423. doi:10.1158/2159-8290.CD-16-1045
- Chacon-Cortes D, Smith RA, Haupt LM, Lea RA, Youl PH, Griffiths LR. Genetic association analysis of miRNA SNPs implicates MIR145 in breast cancer susceptibility. *BMC Med Genet*. 2015;16(1): 107. doi:10.1186/s12881-015-0248-0
- Wu H, Ye C, Ramirez D, Manjunath N. Alternative processing of primary microRNA transcripts by Drosha generates 5' end variation of mature microRNA. *PLoS One*. 2009;4(10):e7566. doi:10.1371/journal.pone.0007566
- Kim B, Jeong K, Kim VN. Genome-wide mapping of DROSHA cleavage sites on primary microRNAs and noncanonical substrates. *Mol Cell*. 2017;66(2):258-269. doi:10.1016/j.molcel.2017.03.013
- Roden C, Gaillard J, Kanoria S. Novel determinants of mammalian primary microRNA processing revealed by systematic evaluation of hairpin-containing transcripts and human genetic variation. *Genome Res*. 2017;27(3):374-384. doi:10.1101/gr.208900.116
- Kwon SC, Baek SC, Choi YG. Molecular basis for the single-nucleotide precision of primary microRNA processing. *Mol Cell*. 2019;73(3):505-518. doi:10.1016/j.molcel.2018.11.005
- Gu S, Jin L, Zhang Y. The loop position of shRNAs and pre-miRNAs is critical for the accuracy of dicer processing In vivo. *Cell*. 2012;151(4): 900-911. doi:10.1016/j.cell.2012.09.042
- Zhu L, Kandasamy SK, Fukunaga R. Dicer partner protein tunes the length of miRNAs using base-mismatch in the pre-miRNA stem. *Nucleic Acids Res*. 2018;46(7):3726-3741. doi:10.1093/nar/gky043
- Jones MR, Quinton LJ, Blahna MT. Zcchc11-dependent uridylation of microRNA directs cytokine expression. *Nat Cell Biol*. 2009;11(9): 1157-1163. doi:10.1038/ncb1931
- Yamane D, Selitsky SR, Shimakami T, et al. Differential hepatitis C virus RNA target site selection and host factor activities of naturally occurring miR-122 3' variants. *Nucleic Acids Res*. 2017;45:4743-4755. doi:10.1093/nar/gkw1332
- Yu F, Pillman KA, Neilsen CT. Naturally existing isoforms of miR-222 have distinct functions. *Nucleic Acids Res*. 2017;45(19):11371-11385. doi:10.1093/nar/gkx788
- Khudayberdiev SA, Zampa F, Rajman M, Schrott G. A comprehensive characterization of the nuclear microRNA repertoire of post-mitotic neurons. *Front Mol Neurosci*. 2013;6:6. doi:10.3389/fnmol.2013.00043
- Koppers-Lalic D, Hackenberg M, Bijnsdorp I. Nontemplated nucleotide additions distinguish the small RNA composition in cells from exosomes. *Cell Rep*. 2014;8(6):1649-1658. doi:10.1016/j.celrep.2014.08.027
- Katoh T, Sakaguchi Y, Miyauchi K. Selective stabilization of mammalian microRNAs by 3' adenylation mediated by the cytoplasmic poly(a) polymerase GLD-2. *Genes Dev*. 2009;23(4):433-438. doi:10.1101/gad.1761509
- Burns DM, D'Ambrogio A, Nottrott S, Richter JD. CPEB and two poly(a) polymerases control miR-122 stability and p53 mRNA translation. *Nature*. 2011;473(7345):105-108. doi:10.1038/nature09908
- Calura E, Ciciani M, Sambugaro A. Transcriptional characterization of stage I epithelial ovarian cancer: a multicentric study. *Cell*. 2019;8(12): 1554. doi:10.3390/cells8121554
- Kurman RJ. *International Agency for Research on Cancer*. 4th ed. Lyon, France: World Health Organization; 2014.

29. Didion JP, Martin M, Collins FS. Atropos: specific, sensitive, and speedy trimming of sequencing reads. *PeerJ*. 2017;5:e3720. doi:[10.7717/peerj.3720](https://doi.org/10.7717/peerj.3720)
30. Langmead B, Trapnell C, Pop M, Salzberg SL. Ultrafast and memory-efficient alignment of short DNA sequences to the human genome. *Genome Biol*. 2009;10(3):R25. doi:[10.1186/gb-2009-10-3-r25](https://doi.org/10.1186/gb-2009-10-3-r25)
31. Desvignes T, Loher P, Eilbeck K, et al. Unification of miRNA and iso-miR research: the mirGFF3 format and the mirtop API. *Bioinformatics*. 2020;36(3):698-703. doi:[10.1093/bioinformatics/btz675](https://doi.org/10.1093/bioinformatics/btz675)
32. Kozomara A, Birgaoanu M, Griffiths-Jones S. miRBase: from micro-RNA sequences to function. *Nucleic Acids Res*. 2019;47(D1):D155-D162. doi:[10.1093/nar/gky1141](https://doi.org/10.1093/nar/gky1141)
33. Lorena Pantano and Georgia Escaramis. isomiRs: analyze isomiRs and miRNAs from small RNA-seq. R package version 1.18.1; 2021.
34. Risso D, Ngai J, Speed TP, Dudoit S. Normalization of RNA-seq data using factor analysis of control genes or samples. *Nat Biotechnol*. 2014;32(9):896-902. doi:[10.1038/nbt.2931](https://doi.org/10.1038/nbt.2931)
35. Robinson MD, McCarthy DJ, Smyth GK. edgeR: a Bioconductor package for differential expression analysis of digital gene expression data. *Bioinformatics*. 2010;26(1):139-140. doi:[10.1093/bioinformatics/btp616](https://doi.org/10.1093/bioinformatics/btp616)
36. Kertesz M, Iovino N, Unnerstall U, Gaul U, Segal E. The role of site accessibility in microRNA target recognition. *Nat Genet*. 2007;39(10):1278-1284. doi:[10.1038/ng2135](https://doi.org/10.1038/ng2135)
37. Wu T, Hu E, Xu S. clusterProfiler 4.0: a universal enrichment tool for interpreting omics data. *Innovation*. 2021;2(3):100141. doi:[10.1016/j.xinn.2021.100141](https://doi.org/10.1016/j.xinn.2021.100141)
38. Poell JB, Mendeville M, Sie D, Brink A, Brakenhoff RH, Ylstra B. ACE: absolute copy number estimation from low-coverage whole-genome sequencing data. *Bioinformatics*. 2019;35(16):2847-2849. doi:[10.1093/bioinformatics/bty1055](https://doi.org/10.1093/bioinformatics/bty1055)
39. Tong Z, Cui Q, Wang J, Zhou Y. TransmiR v2.0: an updated transcription factor-microRNA regulation database. *Nucleic Acids Res*. 2019;47(D1):D253-D258. doi:[10.1093/nar/gky1023](https://doi.org/10.1093/nar/gky1023)
40. Ahn G, Folkins AK, McKenney JK, Longacre TA. Low-grade serous carcinoma of the ovary: clinicopathologic analysis of 52 invasive cases and identification of a possible noninvasive intermediate lesion. *Am J Surg Pathol*. 2016;40(9):1165-1176. doi:[10.1097/PAS.0000000000000693](https://doi.org/10.1097/PAS.0000000000000693)
41. Vang R, Shih IM, Kurman RJ. Fallopian tube precursors of ovarian low- and high-grade serous neoplasms. *Histopathology*. 2013;62(1):44-58. doi:[10.1111/his.12046](https://doi.org/10.1111/his.12046)
42. Löhmußaar K, Kopper O, Korving J, et al. Assessing the origin of high-grade serous ovarian cancer using CRISPR-modification of mouse organoids. *Nat Commun*. 2020;11(1):2660. doi:[10.1038/s41467-020-16432-0](https://doi.org/10.1038/s41467-020-16432-0)
43. Babaier A, Mal H, Alselwi W, Ghatage P. Low-grade serous carcinoma of the ovary: the current status. *Diagnostics*. 2022;12(2):458. doi:[10.3390/diagnostics12020458](https://doi.org/10.3390/diagnostics12020458)
44. Kandimalla R, Wang W, Yu F, et al. OCaMIR-A noninvasive, diagnostic signature for early-stage ovarian cancer: a multi-cohort retrospective and prospective study. *Clin Cancer Res Off J Am Assoc Cancer Res*. 2021;27(15):4277-4286. doi:[10.1158/1078-0432.CCR-21-0267](https://doi.org/10.1158/1078-0432.CCR-21-0267)
45. Qi X, Yu C, Wang Y, Lin Y, Shen B. Network vulnerability-based and knowledge-guided identification of microRNA biomarkers indicating platinum resistance in high-grade serous ovarian cancer. *Clin Transl Med*. 2019;8(1):28. doi:[10.1186/s40169-019-0245-6](https://doi.org/10.1186/s40169-019-0245-6)
46. Benvenuto G, Todeschini P, Paracchini L, et al. Expression profiles of PRKG1, SDF2L1 and PPP1R12A are predictive and prognostic factors for therapy response and survival in high-grade serous ovarian cancer. *Int J Cancer*. 2020;147(2):565-574. doi:[10.1002/ijc.32935](https://doi.org/10.1002/ijc.32935)
47. Ferreira P, Roela RA, Lopez RVM, Del Pilar E-DM. The prognostic role of microRNA in epithelial ovarian cancer: a systematic review of literature with an overall survival meta-analysis. *Oncotarget*. 2020;11(12):1085-1095. doi:[10.18632/oncotarget.27246](https://doi.org/10.18632/oncotarget.27246)
48. Jacques C, Tesfaye R, Lavaud M. Implication of the p53-related miR-34c, -125b, and -203 in the osteoblastic differentiation and the malignant transformation of bone sarcomas. *Cell*. 2020;9(4):810. doi:[10.3390/cells9040810](https://doi.org/10.3390/cells9040810)
49. Achari C, Winslow S, Ceder Y, Larsson C. Expression of miR-34c induces G2/M cell cycle arrest in breast cancer cells. *BMC Cancer*. 2014;14(1):538. doi:[10.1186/1471-2407-14-538](https://doi.org/10.1186/1471-2407-14-538)
50. Hagman Z, Larne O, Edsjö A, et al. miR-34c is downregulated in prostate cancer and exerts tumor suppressive functions. *Int J Cancer*. 2010;127(12):2768-2776. doi:[10.1002/ijc.25269](https://doi.org/10.1002/ijc.25269)
51. Wu Z, Wu Y, Tian Y. Differential effects of miR-34c-3p and miR-34c-5p on the proliferation, apoptosis and invasion of glioma cells. *Oncol Lett*. 2013;6(5):1447-1452. doi:[10.3892/ol.2013.1579](https://doi.org/10.3892/ol.2013.1579)
52. Liu F, Wang X, Li J. miR-34c-3p functions as a tumour suppressor by inhibiting eIF4E expression in non-small cell lung cancer. *Cell Prolif*. 2015;48(5):582-592. doi:[10.1111/cpr.12201](https://doi.org/10.1111/cpr.12201)
53. Yan M, Yang X, Shen R, et al. miR-146b promotes cell proliferation and increases chemosensitivity, but attenuates cell migration and invasion via FBXL10 in ovarian cancer. *Cell Death Dis*. 2018;9(11):1123. doi:[10.1038/s41419-018-1093-9](https://doi.org/10.1038/s41419-018-1093-9)
54. Wang Y, Zhao S, Zhu L, Zhang Q, Ren Y. MiR-19a negatively regulated the expression of PTEN and promoted the growth of ovarian cancer cells. *Gene*. 2018;670:166-173. doi:[10.1016/j.gene.2018.05.063](https://doi.org/10.1016/j.gene.2018.05.063)
55. Chen X, Yang F, Zhang T. MiR-9 promotes tumorigenesis and angiogenesis and is activated by MYC and OCT4 in human glioma. *J Exp Clin Cancer Res*. 2019;38(1):99. doi:[10.1186/s13046-019-1078-2](https://doi.org/10.1186/s13046-019-1078-2)

SUPPORTING INFORMATION

Additional supporting information can be found online in the Supporting Information section at the end of this article.

How to cite this article: Velle A, Pesenti C, Grassi T, et al. A comprehensive investigation of histotype-specific microRNA and their variants in Stage I epithelial ovarian cancers. *Int J Cancer*. 2023;152(9):1989-2001. doi:[10.1002/ijc.34408](https://doi.org/10.1002/ijc.34408)